Clim. Past Discuss., 9, 4553–4598, 2013
www.clim-past-discuss.net/9/4553/2013/
doi:10.5194/cpd-9-4553-2013
© Author(s) 2013. CC Attribution 3.0 License.

Climate of the Past Discussions
Open Access

This discussion paper is/has been under review for the journal Climate of the Past (CP).
Please refer to the corresponding final paper in CP if available.

Qualitative and quantitative reconstruction of surface water characteristics and recent hydrographic changes in the Trondheimsfjord, central Norway

G. Milzer[1], J. Giraudeau[1], S. Schmidt[1], F. Eynaud[1], and J. Faust[2]

[1]EPOC, Université de Bordeaux, CNRS, UMR5805, Talence, France
[2]Geological Survey of Norway (NGU), Trondheim, Norway

Received: 30 July 2013 – Accepted: 2 August 2013 – Published: 13 August 2013

Correspondence to: G. Milzer (g.milzer@epoc.u-bordeaux1.fr)

Published by Copernicus Publications on behalf of the European Geosciences Union.

Abstract

In the present study we investigate dinocyst assemblages in the Trondheimsfjord over the last 25 to 50 yr from three well-dated multi-cores (^{210}Pb and ^{137}Cs) retrieved along the fjord axis. The downcore distribution of the cysts is discussed in view of changes of the key surface water parameters sea-surface temperatures (SSTs) and sea-surface salinities (SSSs) monitored in the fjord, as well as river discharges. We examine the impact of the North Atlantic Oscillation pattern and of waste water supply from the local industry and agriculture on the fjord ecological state and hence dinocyst species diversity. Our results show that dinocyst production and diversity in the fjord is not evidently affected by human-induced eutrophication. Instead the assemblages appear to be mainly controlled by the NAO-related changes in physico-chemical characteristics of the surface mixed layer. Still, discharges of major rivers were modulated, since 1985 by the implementation of hydropower plants which certainly influences the freshwater and nutrient supply into the fjord. The impact, however, is variable according to the local geographical setting, and barely differentiated from natural changes in river run off.

We ultimately test the use of the modern analogue technique (MAT) for the reconstruction of winter and summer SSTs and SSSs and annual primary productivity (PP) in this particular fjord setting. The reconstructed data are compared with time-series of SSTs and SSSs measured at 10 m water depth, as well as with mean annual PPs along the Norwegian coast and within Scandinavian fjords. The reconstructions are in general good agreement with the instrumental measurements and observations from other fjords. Major deviations can be addressed to peculiarities in the assemblages linked to the particular fjord setting and the related hydrological structure.

CPD
9, 4553–4598, 2013

1 Introduction

The climate of western Norway is closely coupled to the circulation of the topographically-steered North Atlantic Current (NAC) and Norwegian Coastal Current (NCC) flowing northward along the continental margin over the Norwegian shelf (Loeng and Drinkwater, 2007). The lateral distribution and physico-chemical characteristics of the NCC, which is supplied by brackish water from the Baltic Sea, rivers and fjords along the Norwegian coast, are linked to the prevailing wind patterns in the North Atlantic realm (Sætre, 1999, 2007). The Trondheimsfjord in western central Norway adjoins the Norwegian Sea. The fjord hydrology is similarly coupled to the NAC and NCC circulation, as well as to local riverine input from the hinterland (Sakshaug and Myklestad, 1973; Jacobson, 1983). Fjords are relatively sheltered environments where biogenic and lithogenic sediments accumulate at very high rates (Howe et al., 2010). The fjord sediments and incorporated fossil microorganisms therefore provide highly resolved information on temporal changes of the fjord hydrology related to the proximal ocean current variability, and on the interaction of marine and continental climate conditions.

The distribution of the dinoflagellate cysts (or dinocysts), the zygotic products of dinoflagellates, in sediments is controlled by the surface water characteristics making them widely used as paleoceanographic proxies for the reconstruction of sea-surface parameters (e.g. Harland, 1983; de Vernal et al., 1993; Rochon et al., 1999; Marret and Zonneveld, 2003; Zonneveld et al., 2013). Dinocysts are composed of highly resistant refractory organic matter and are therefore usually well preserved in sediments (e.g. Rochon et al., 1999; de Vernal et al., 2000). Dinoflagellates in coastal environments are generally adapted to large sea-surface temperature (SST) and salinity (SSS) ranges due to the seasonally varying relative influence of marine/coastal and continental waters. In these settings their occurrence is therefore rather related to other species-discriminating environmental parameters than in the open ocean, such as lateral and vertical salinity gradients, nutrient availability and the species-specific ability to adapt to

CPD
9, 4553–4598, 2013

rapidly changing hydrological conditions (e.g. Smayda and Reynolds, 2003; Harland et al., 2004, 2006; Radi et al., 2007; Pospelova et al., 2010). These hydrological changes may however be biased by local and regional anthropogenically induced changes in the coastal and fjord environment (Sætre et al., 1997; Dale, 2001). Recent studies on surface sediments from the Trondheimsfjord which encompass the past 4–20 yr, show large spatial variability in the composition of cyst assemblages linked to the complex fjord hydrography and topography (Milzer et al., 2013). Untreated waste water from local and regional industry and agriculture was directly led into the Trondheimsfjord until 1980. The assemblages, however, do not reveal any indications of human-induced eutrophication suggesting that recently imposed environmental regulations and restrictions to reduce these nutrient inputs were highly effective (Tangen and Arff, 2003). Alternatively, the exchange of Trondheimsfjord waters with the open sea strongly dilutes excess nutrient loads, and the regular supply of oxygen-rich Atlantic waters prevents hypoxic or anoxic conditions at the bottom (Tangen and Arff, 2003).

In the following study we investigate recent changes in the dinocyst assemblages in the Trondheimsfjord over the last 25 to 50 yr from three sediment cores located along the fjord axis. We discuss the downcore distribution of dinocysts in view of naturally and anthropogenically induced changes with regard to SST and SSS variability (monitored at three fixed mooring stations in the fjord), annual mean river discharges, atmospheric oscillation patterns (state of the North Atlantic Oscillation – NAO) and nutrient availability which all together account for changes of the fjord ecological state (Sakshaug and Myklestad, 1973; Ottersen et al., 2001). We ultimately apply the now standard Modern Analogue Technique (MAT) to the downcore distribution of dinocysts and test its ability to quantitatively reconstruct a series of sea-surface parameters (SST, SSS and primary productivity (PP)) in this fjord setting, in order to establish a solid basis for the future investigation of Holocene paleoclimate and paleoceanographic variability.

CPD
9, 4553–4598, 2013

2 Physical settings and modern hydrology

The Trondheimsfjord extends from 63°40′ N/9°45′ E at Ørland at the fjord entrance to 64°45′ N/11°30′ E at the fjord head at Verdal (Jacobson, 1983, and references therein), and runs over into the Beitstadfjord from Skarnsund 63°50′ N/11°04′ E until Steinkjer at 63°00′ N/11°28′ E (Fig. 1). The fjord is 135 km long with an overall volume of 235 km^3 and a surface area of 1420 km^2 (Jacobson, 1983). The entire fjord area is divided into three basins, the Seaward Basin, the Middle Fjord and the Beitstadfjord. The basins are separated by three sills located at the fjord entrance (217 m water depth), at the island of Tautra (77 m water depth), and at Skarnsund (140 m water depth) (Fig. 1) (Ellingsen, 2004, and references therein). Sediment deposition in the Trondheimsfjord is largely controlled by the prevalent currents and the associated pelagic/marine sediment load, the topography and rivers delivering large amounts of terrigenous sediment to the fjord (Bøe et al., 2003; Milzer et al., 2013). Bottom currents and tidal currents in the subsurface layers prevent the rapid deposition of the fine particle fraction in topographically elevated areas as sills, and trigger the sediment remobilisation across the fjord. Sedimentation rates are consequently higher in the sheltered fjord basins such as Middle Fjord and Beitstadfjord than at the fjord entrance and in the Seaward Basin where several currents pass at high frequencies (Bøe et al., 2003; Milzer et al., 2013).

2.1 Water mass exchange with the Norwegian Sea

The hydrology of the Trondheimsfjord is characterized by a three layer system mainly driven by density differences related to the seasonal temperature and salinity variability of the water masses inside and outside the fjord (e.g. Sakshaug and Myklestad, 1973; Strømgren, 1974; Jacobson, 1983). The bottom water is generally renewed twice a year, in February–June and September–November, by NAC and NCC waters, respectively (Sakshaug and Myklestad, 1973; Strømgren, 1974; Jacobson, 1983). The depth of the NAC and its ability to cross the sill at the Trondheimsfjord entrance depends on the depth of the overlying wedge-shaped NCC which, in turn, is linked to the prevailing

CPD
9, 4553–4598, 2013

seasonal wind patterns in the Nordic Seas (Jacobson, 1983; Sætre, 1999, 2007). In early winter–spring, when the NCC is supplied by large amounts of fresh water from the Norwegian hinterland, the current is deflected offshore by northerly winds forming a shallow surface layer. NAC waters replace the NCC at lower depths, cross the sill at the fjord entrance and renew the fjord bottom water. In late summer/early autumn, south westerly winds induce a downwelling of the NCC inhibiting the crossing of NAC waters over the sill. Consequently, NCC waters substitute the fjord water at intermediate depth (e.g. Sakshaug and Myklestad, 1973; Jacobson, 1983).

The intermediate/subsurface and surface waters in the Trondheimsfjord are subject to a two-layer estuarine circulation induced by large amounts of fresh water supplied by the 6 major rivers Orkla, Gaula, Nidelva, Stjørdalselva, Verdalselva and Steinkjerelva (Fig. 1) with a mean annual runoff of 725 $m^3 s^{-1}$ and up to 6430 $m^3 s^{-1}$ during spring (Ellingsen, 2004 and references therein; Pettersson, 2012). Tidal surface currents are considered to be the main force for internal mixing with a semidiurnal sea level change of ca. 1.8 m (Jacobson, 1983). The tidal currents flow anti-clockwise, entering the fjord on its southern edge during flood and flowing out along the northern edge during ebb (Jacobson, 1983).

2.2 Surface water characteristics over the past 50 yr

The temperature and salinity structure and the nutrient content in the surface waters vary seasonally linked to coastal water exchange, riverine input and internal mixing (Sakshaug and Myklestad, 1973; Strømgren, 1974; Jacobson, 1983). These water mass characteristics, in turn, are to a large extent controlled by the prevailing winter NAO pattern of atmospheric variability (Ottersen et al., 2001). During a positive NAO-phase, the Norwegian climate is dominated by marine warm and wet air masses from lower latitudes causing strong precipitation and continental run-off (e.g. Hurrell and van Loon, 1997; Ottersen et al., 2001). During a negative oscillation state, Norway is affected by pulses of cold and dry continental air masses resulting in extremely low temperatures and reduced continental run-off. This atmospheric influence explains

CPD
9, 4553–4598, 2013

to a high extent the modern mean annual SST and SSS variability over the Norwegian margin and the adjoining coastal systems (Visbeck et al., 2003; Blindheim et al., 2000). Contrary to the deep water layers, which are largely decoupled from the surface layers after the bottom water exchange, SSTs and SSSs strongly vary seasonally and (multi)annually in the Trondheimsfjord (Jacobson, 1983). According to instrumental measurements obtained from mooring stations within the Trondheimsfjord (Fig. 2), SSSs and SSTs at 10 m water depth display a minor long term salinity decrease (< 0.5 PSU) and temperature increase (ca. 1 °C) over the past 42 yr (data from Trondhjem Biological Station of the Norwegian University of Science and Technology (NTNU): http://www.ntnu.edu/biology/tbs). On an annual to decadal scale, mean annual river discharges (data from Norwegian Water Resources and Energy Directorate (NVE): www.nve.no) are lowest when the NAO is in its negative state and highest during a positive oscillation phase. This NAO-forced variability in river discharges is concomitant with the SST and SSS fluctuations with increased consistency towards the inner fjord (Fig. 2). Calculated correlation coefficients between the NAO-index, river discharge, SST and SSS are highest during spring and autumn (R^2 = 0.6–0.9). Annual to multiannual SST changes closely correspond to the NAO pattern in winter (R^2 = 0.6–0.9) suggesting a major influence of atmospheric temperatures on the thermal signature of the surface waters. Still, the close relationship between NAO phases and SST and SSS changes seems to be best established before 1980. This might be either explained by the long term negative NAO phase until ca. 1982, which imposed a higher climatic stress on the fjord surface water, or, alternatively, by the implementation of local hydropower plants in the early 80s' such as in the Orkla river which modifies the river input (L'Abée-Lund et al., 2009) (Fig. 2).

A proper investigation of the NAO impact (and associated precipitation and atmospheric temperature changes) on the quantity and type of nutrients in the fjord surface mixed layer is not possible yet, due to the lack of time series of nutrient concentrations. Short-term observations by Sakshaug and Myklestad (1973) in 1970/71, however, showed that nutrients such as nitrite, nitrate, orthophosphate and silicate,

CPD
9, 4553–4598, 2013

fluctuate seasonally according to the depth and stability of the pycnocline and riverine input. The supply of NO_3-N and PO_4-P to the Seaward Basin from continental run off and rivers roughly amounted to 1.2–7.0 tons day^{-1} and below 0.15 tons day^{-1}, respectively, with maxima in late spring and autumn. Sewage supplied directly to the outer fjord yielded ca. 2.5 and 0.75 tons daily of total N and total P, respectively (Sakshaug and Myklestad, 1973).

3 Material and methods

Three sediment cores were retrieved along the fjord axis, in Stjørnfjord at the fjord entrance, in the central Seaward Basin and in the Middle Fjord (Fig. 1, Table 1) with a multi-corer as part of a research cruise of the research vessel FF Seisma from the Geological Survey of Norway (NGU) in April 2011. The sediment cores were sub-sampled on board at 1 cm intervals and split into two halves later in the lab, one for radiometric dating and one for dinocyst census counts. The sediment samples were freeze-dried in order to save as much material as possible for dinocyst census counts.

3.1 Chronology and sediment accumulation rates

Activities of ^{210}Pb, ^{226}Ra, ^{137}Cs and ^{232}Th were measured in ca. 4–5 g of dried bulk sediment using a low background, high efficiency, well-shaped γ-detector (Schmidt et al., 2013). Activities are expressed in mBq g^{-1} and errors correspond to 1 SD counting statistics. The detector was calibrated using IAEA standards (RGU-1; RGTh; SOIL-6). Excess of ^{210}Pb (^{210}Pb$_{xs}$) was calculated as the difference of the total activity of ^{210}Pb in the sediment and the supported activity by its parent isotope ^{226}Ra. The error on ^{210}Pb$_{xs}$ therefore corresponds to the propagation of errors in measured ^{210}Pb and ^{226}Ra activities.

The dating of the multi cores relies on ^{210}Pb, a naturally-occurring radionuclide in the sediment with a half-live of 22.3 yr. This method is commonly used to estimate

CPD
9, 4553–4598, 2013

short-term (years to decades) sediment accumulation rates in continental and oceanic environments for the last 40 yr (Appleby, 2001). Briefly, dating is calculated using the excess activity of ^{210}Pb (^{210}Pb$_{xs}$) which derives from atmospheric fallout and water column scavenging, and is rapidly incorporated into the sediment. The unsupported ^{210}Pb incorporated in the sediment decays with time according to its half-live. In order to estimate ages and/or sediment accumulation rates several models have been developed assuming different hypothesis such as constant initial concentration (CIC model), constant rate of supply (CSR model) or constant flux and constant sedimentation (CF : CS model) (Kirchner, 2011, among others). In this study we applied the CF : CS model and examined its accuracy in dating of the sedimentary archives using ^{137}Cs ($T_{1/2}$ = 30 yr) (e.g. Robbins and Edgington, 1975; Durantou et al., 2012). This artificial radionuclide serves as independent time-stratigraphic marker due to elevated activity peaks associated with nuclear weapon test fallouts (maximum in 1963) and the Chernobyl accident in 1986 (Durantou et al., 2012).

3.2 Dinocysts: sample preparation and ecological background

Dinoflagellate cysts were retrieved from the < 150 µm fraction. The treatment of the samples follows a standard sample preparation procedure (e.g. Stockmarr, 1971; de Vernal et al., 1996), slightly modified at EPOC/Université Bordeaux1 (Penaud et al., 2008, http://www.epoc.u-bordeaux.fr/index.php?lang=fr&page=eq_paleo_pollens). The samples were treated with cold hydrochloric acid (HCL) (10, 25 and 50 %) and cold 40 and 70 % hydrogen fluoride (HF) to dissolve carbonates and silicates and washed through a 10 mm nylon mesh. The residue was centrifuged and additionally swirled in a large watch glass to remove high amounts of amorphous organic material (AOM) (Riding and Kyffin-Hughes, 2004; Milzer et al., 2013). The final residue was mounted with glycerine jelly between the microscope slides. On average, 300 cysts per slide were counted using a Zeiss Axioscope light microscope at 40× magnification. Absolute abundances (cysts cm^{-3}) of dinocysts and palynomorphs were calculated

CPD
9, 4553–4598, 2013

using the *Lycopodium* marker grain method (Stockmarr, 1971). Relative abundances (%) of each species were calculated including only dinoflagellate cysts.

The taxonomical nomenclature corresponds to Rochon et al. (1999) and Head et al. (2001, 2006). *Operculodinium centrocarpum s.l.* includes the long and short-process forms of *O. centrocarpum sensu* (Wall and Dale, 1967) and *O. centrocarpum* – Arctic morphotype (de Vernal et al., 2001). Dinocyst species within the *Spiniferites*, *Selenopemphix*, *Islandinium*, *Brigantedinium* and *Impagidinium* groups were grouped according to Marret and Zonneveld (2003), as summarized in Milzer et al. (2013). The resulting species richness in the studied sediment cores from the Trondheimsfjord amounted to a maximum of 17 dinocyst taxa and 4 chlorophycean and Prasinophyceae species. The spatial distribution of the dominant species in surface sediments of the Trondheimsfjord was recently discussed by Milzer et al. (2013). The following section summarizes the ecology and environmental background of each recognized species. Unless otherwise specified, most information are taken from Matthiessen (1995), Rochon et al. (1999), Marret and Zonneveld (2003), de Vernal and Marret (2007), van Nieuwenhove et al. (2008), and Zonneveld et al. (2013).

The autotrophic species *Pentapharsodinium dalei* is associated with cold and stratified waters as typical for Norwegian fjords and other temperate and polar embayments. This species generally blooms in spring – early summer when it takes advantage of enhanced amounts of nutrients in the water column from previous winter mixing, of increasing stability of the water column and of rising amounts of sun light (Grøsfjeld et al., 1999; Grøsfjeld and Harland, 2001). *Operculodinium centrocarpum* is considered as a cosmopolitan species which is able to quickly adapt to environmental changes, and is therefore often observed in coastal waters and/or at the coastal/oceanic boundary (Wall and Dale 1967; Dale et al., 2002, 1999b). In the Nordic Seas this species is associated with the pathway of the warm and saline NAC (de Vernal et al., 2000). *Selenopemphix quanta* s.l. is a heterotrophic species which has been mainly documented from subtropical coastal areas in regions characterized by mesotrophic to eutrophic conditions. The abundance of the heterotrophic species *Brigantedinium* spp.

CPD
9, 4553–4598, 2013

largely depends on the presence of diatom preys whose occurrence is similarly linked to nutrient enrichment in the photic layer. The heterotrophic taxon *Islandinium minutum* shows a bipolar distribution in coastal areas north of 30° N and south of 30° S, withstanding large (inter-)seasonal fluctuations of temperature, salinity, insolation, nutrient concentration, and sea-ice cover. Cysts of *Lingulodinium machaerophorum* are reported to be restricted to regions with summer temperatures above 10–12 °C. An enhanced occurrence of *L. machaerophorum* in southern Norwegian fjords has been related to eutrophication due to industrial and agricultural activity (Sætre et al., 1997; Dale et al., 1999a) as well as frequently to increased freshwater advections (Zaragosi et al., 2001). *Ataxiodinium choane* is a coastal to open oceanic fully marine species with highest relative abundances in eutrophic environments (Marret et al., 2004). In this study the species is most likely related to an enhanced influence of Atlantic-derived waters. Cysts of *Nematosphaeropsis labyrinthus* are generally linked to outer neritic to oceanic environments and to eutrophic conditions within the North Atlantic Ocean (Devillers and de Vernal, 2000). The *Spiniferites* group is dominated by *Spiniferites ramosus* and *Spiniferites elongatus*. *Spiniferites ramosus s.l.* is considered as a cosmopolitan species linked to upwelling or a well-mixed surface water layer resulting in mesotrophic to eutrophic conditions. Nowadays highest occurrence of *S. elongatus s.l.* is found around Iceland, potentially indicating a preference to colder and lower salinity but eutrophic surface water conditions (Marret et al., 2004). Cysts of *Spiniferites lazus*, *Spiniferites mirabilis*, *Spiniferites membracaneus*, *Spiniferites delicatus* and *Spiniferites bentorii* are associated with marine warm and saline waters in oligo-/mesotrophic environments. Since their total abundance in the Trondheimsfjord does not exceed 3 % we relate their presence to a stronger marine influence in surface layers assigned as the combined term *Spiniferites "AW"* without distinguishing their particular species-specific characteristics. All species grouped within *Impagidinium ssp.* generally thrive in fully marine environments (rarely neritic) with oligotrophic to eutrophic conditions. The distribution of *Bitectatodinium tepikiense* is related to the transitional zone between the subpolar and temperate zones in the Norwegian Sea (Grøsfjeld and Harland, 2001). Higher

CPD
9, 4553–4598, 2013

abundances of this species may indicate a strong seasonal temperature gradient with enhanced surface water stratification. Cysts of *Polykrikos schwartzii* do not seem to be restricted to coastal areas and they are generally found in sediments from subtropical to temperate continental shelves, estuaries and shelf seas of the North Sea, Skagerrak/Kattegat, the North Atlantic and Greenland Sea and Nordic Seas. Cysts of *Alexandrium tamarense* are reported in coastal sediments of temperate/subtropical regions with brackish to fully marine, oligotrophic to eutrophic environments from the coasts of e.g. Germany, Sweden, and Spain (Nehring et al., 1997 and references therein). The increased abundance of *Halodinium minor*, *Radiosperma corbiferum* and *Hexasteria problematica* is related to moderate salinity and high nutrient content in surface waters in transitional brackish to marine environments (e.g. Parke and Dixon, 1964; McMinn, 1991; Matthiessen, 1995; Sorrel et al., 2006; Price and Pospelova, 2011).

3.3 Multivariate analyses

Multivariate analyses were applied on the relative cyst abundancesin in order to extract major patterns in species abundances, and to investigate their spatio-temporal organization according to the various geographical and environmental settings of the studied sediment cores. The analyses were conducted using the free software package RStudio (integrated development environment for R, Version 0.97.336) and the paleontological statistics software "PAST" (http://folk.uio.no/ohammer/past/) by Hammer et al. (2001). We performed a statistically based classification of the investigated sediment samples into groups based on species assemblages (species relative abundances) using non-metric multidimensional scaling (NMDS) and the Bray-Curtis (dis)similarity index visualized in a two-dimensional space. The grouping was conducted on both separate data sets related to single sediment cores, and on the combined cyst assemblages obtained from the three studied multi-cores. The Shepard plot was applied as a quality/reliability measure of the grouping (Holland, 2008). In a final step we performed a correspondence analysis (CA) on the combined three data sets of cyst abundances to define groups in terms of characteristic species, and

CPD
9, 4553–4598, 2013

to discuss them with regard to the geographical, environmental and stratigraphical contexts controlling the cyst distribution (Hammer et al., 2001).

3.4 Quantitative reconstructions of the sea-surface parameters SST, SSS and PP

The modern analogue technique (MAT) was applied to the relative cyst abundances in the studied sediment cores for quantitative reconstructions of winter and summer SSS and SST, and annual primary productivity (PP) (de Vernal et al., 2001; Radi and de Vernal, 2004; Guiot and de Vernal, 2007). Hydrographical (summer and winter SST and SSS) and annual primary productivity data at 0 m water depth averaged over the period 1900 to 2001 (NODC, 2001), and 2002 to 2005 (VGP model applied on MODIS chlorophyll data), respectively, were assigned to each of the reference modern sites (i.e. analogues). Sea surface conditions were then reconstructed for the fossil records based on their similarity with the modern dinocyst spectra. The corresponding hydrographical data were obtained by a weighted average of the 5 best analogues (maximum weight is given for the closest analogue in terms of statistical distance). The accuracy of the approach is assessed by the correlation coefficient between observed and estimated values for each reconstructed parameter when the test is performed on the calibration data set (i.e. the modern database excluding the spectrum to analyze, see de Vernal et al., 2001, 2005). This step furthermore provides residual differences between observations and estimates from which is derived the root mean square error (RMSE) of prediction, equivalent to the standard deviation of these residuals (e.g. de Vernal et al., 2001, 2005; Radi and de Vernal, 2004; Guiot and de Vernal, 2007).

The MAT was run using the free R software (http://www.r-project.org/) with a script especially developed by J. Guiot in the BIOINDIC package (https://www.eccorev.fr/spip.php?article389). The reconstructions of winter and summer SSTs and SSSs as well as PPs were achieved using the original dataset of Radi and de Vernal (2008) collected in the Northern Hemisphere of the North Atlantic, Arctic and North Pacific Ocean with additional data points (database available from the DINO9 workshop, http://pcwww.liv.

CPD
9, 4553–4598, 2013

ac.uk/~dino9/workshops.htm), bringing the total number of sites to 1207. Most accurate reconstructions (based on linear regressions of estimated vs. observed data) can be achieved for winter and summer SSTs with $R^2 = 0.98$ and RMSE = 1.0 °C, and $R^2 = 0.96$ and RMSE = 1.5 °C, respectively. Summer SSSs similarly reveal a good accuracy with $R^2 = 0.74$ and RMSE = 2.4 PSU. The lowest accuracy was achieved for winter SSSs with $R^2 = 0.69$ and RMSE = 2.3 PSU. The validation test for the reconstruction of primary productivity yields a good accuracy with $R^2 = 0.84$ and quite a large RMSE = 54.6 g C m^{-2} yr^{-1}.

In a final step we compared separately the reconstructed mean, minimum and maximum SST and SSS values with the equivalent measured time series monitored at 10 m water depth at the respective mooring stations (Røberg for core MC 61-1 and MC99-1, Ytterøy for core MC S4-1) and tested the similarity/variance using the Mann–Whitney (Wilcoxon) test (Bigler and Wunder, 2003; von Detten et al., 2008).

4 Results and Discussion

4.1 Chronologies and sediment accumulation rates

$^{210}Pb_{xs}$ activities in MC 99-1, in the Seaward basin, range from 37 to 159 m Bq g^{-1}, decreasing downcore according to the radioactive decay of ^{210}Pb with time (Fig. 3). With regard to the CF : CS model the sediment accumulation rate in MC 99-1 is 0.49 cm yr^{-1} and encompasses the last 49 yr. The counting error increases downcore reaching max. 3.5 yr (Fig. 3). The ^{137}Cs profile in MC 99-1 shows remarkable peak activities with maximum values of 53–59 m Bq g^{-1} at 12–13 cm and of 36–37 m Bq g^{-1} at 23–24 cm sediment depths. According to the $^{210}Pb_{xs}$-based dating, sediments at these depths correspond to an age of 1986 ± 1.7 yr and ca. 1963–1965 ± 3.4 yr, respectively, which is in good agreement with the known nuclear power plant accident in Chernobyl (1986) and the nuclear weapon test fallouts (max. in 1963) (Fig. 3).

CPD
9, 4553–4598, 2013

Activities of $^{210}Pb_{xs}$ at the fjord entrance (core MC 61-1) decrease continuously with depth from 132 to 69 m Bq g^{-1}. The deepest layer of core MC 61-1 (10.5 cm) shows an increase in activity (82 m Bqg^{-1}) with a concomitant increase of ^{232}Th (data not shown). The long-lived ^{232}Th occurs naturally and is usually associated with the detrital fraction. Variations in ^{232}Th activities are thus assumed to trace changes in the detrital fraction proportion (van der Klooster et al., 2011). Sedimentation rate in MC 61-1 was therefore estimated based on $^{210}Pb_{xs}$ activities normalized by the measured ^{232}Th activities to correct for any deviations related to substrate changes (Fig. 3). The corresponding sediment accumulation rate yields 0.46 cm yr^{-1}. The 12 cm long sediment core thus comprises the past 25 yr (± max. 1.1 yr). The time period encompassed in this sedimentary archive is too short to reveal peak activities associated with the Chernobyl accident or past nuclear weapon tests. The absence of activity peaks in ^{137}Cs profile, however, serves as an indirect validation (Fig. 3).

The activities of $^{210}Pb_{xs}$ in MC S4-1 in the Middle Fjord range from 44 to 11 m Bq g^{-1} from the sediment surface to the lowermost depths, with fairly low activities from 11 to 16 m Bq g^{-1} at depths deeper than 28 cm (Fig. 3). The core is located in a deep basin surrounded by hills, and the river Verdalselva discharges significant amounts of fresh water and terrigenous sediments from the hinterland into the Middle Fjord. We assume that relatively low $^{210}Pb_{xs}$ activities as well as the changes in the activity profile below 28 cm sediment depths may be related to changes in sediment source and delivery. We therefore normalized the measured $^{210}Pb_{xs}$ activities with the depth-related activities of the detrital tracers ^{232}Th similarly to the chronology in MC 61-1. The sedimentation rate in the 38 cm long multi-core MC S4-1 yields 0.68 cm yr^{-1} and consequently encompasses the last 55 yr with maximum error of ±5 yr (increasing downcore). Peak activities of ^{137}Cs (54 m Bq g^{-1}) at depths of 16–18 cm (according to the chronology accomplished by correcting for changes in the detrital fraction) correspond to the years 1985–1987 and can thus be addressed to the Chernobyl accident in 1986 (Fig. 3). In depth 31–32 cm the expected peak related to fallout test is not well expressed.

CPD
9, 4553–4598, 2013

However, the occurrence of detectable ^{137}Cs activities testifies for sediments deposited after 1950.

4.2 Dinocyst concentrations and preservation

Palynomorphs identified within the studied cores are mainly dominated by dinocysts whereas Chlorophycean and Prasinophyceae algae account always for less than 5 % of the total assemblages. The following discussion will therefore only relate to dinocysts. Maximum absolute abundances of dinocysts were found in MC 61-1 in Stjørnfjord at the fjord entrance, fluctuating between ca. 10 000 and 130 000 specimens cm^{-3} with mean concentrations of 72 000 specimens cm^{-3} (Fig. 4a). Values were significantly lower in the cores located in Middle Fjord and the Seaward Basin with mean cyst concentrations of 25 000 specimens cm^{-3} (MC S4-1) and 14 000 specimens cm^{-3} (MC 99-1) (Fig. 4a).

These relatively high mean concentrations correspond well with observations by Dale (1976) from a limited set of surface samples, and our own analysis based on 59 surface samples evenly distributed in the Trondheimsfjord (Milzer et al., 2013), as well as to concentrations at inner shelf and fjord environments along the Norwegian coast observed by Grøsfjeld and Harland (2001). Differences in mean cyst concentrations among the studied multi-cores are most likely related to the various sedimentary processes linked to the current circulation features, and to the proximity of river inlets and associated nutrient and terrigenous sediment loads (see Sect. 2). Highest absolute cyst abundance and largest species evenness are observed in MC 61-1 in Stjørnfjord at the fjord entrance and can be related to the proximity of the Norwegian Sea. Stjørnfjord is easily flushed with Atlantic water and is likely to experience a periodical coastal upwelling resulting in an enhanced nutrient availability. Additionally, the dilution of marine biogenic material by terrestrial organic and lithogenic particles might be limited (sediment accumulation is lowest at site MC 61-1 (0.46 cm yr^{-1})) due to lower terrigenous inputs linked to the absence of major river inlets contrary to the inner parts of the Trondheimsfjord. The Seaward basin receives discharges from 4 of

CPD
9, 4553–4598, 2013

the 6 major rivers which end in the Tronsheimsfjord (Fig. 1). Associated nutrient and terrigenous loads as well as dinocysts thriving in the surface layers are distributed across the fjord, linked to the general circulation pattern of the surface currents during flood (Jacobson, 1983). Sediment (sedimentation rate in core MC 99-1: 0.49 cm yr^{-1}) and cyst accumulation in the deep Seaward basin is thus limited despite the proximity of major river inlets. Moreover, the observed low cyst concentrations measured at site MC 99-1 (mean = 14 000 cysts cm^{-3}) might also be explained by strong dilution by sediments carried into the fjord basin during bottom water renewal events. Middle fjord is more sheltered than the Seaward basin with relatively high riverine (and nutrient) input and high sedimentation rates (MC S4-1: 0.68 cm yr^{-1}). Additionally, tidal surface currents cause a drift of cysts towards the fjord head during flood. Cyst concentrations are, nevertheless, relatively low and we assume that cyst assemblages in Middle Fjord are subject to dilution due to the large sediment input from the hinterland.

Ultimately, the preservation ability against post-depositional degradation due to sediment oxygenation may alter the original cyst assemblages (Zonneveld et al., 1997, 2001). The dominant species in the Trondheimsfjord, *P. dalei*, is considered to be relatively resistant to aerobic decay (Zonneveld et al., 1997, 2008), in contrast to the moderately sensitive cysts of *O. centrocarpum, L. machaerophorum,* and the highly sensitive *Brigantedinium spp.* species. Post-depositional degradation may therefore partly cause the poor cyst evenness and species dominance in the fjord sediments. Still, the relatively high sedimentation rates are supposed to limit degradation processes by minimizing the time organic remains are exposed to oxygen in the bottom and pore waters.

4.3 Species diversity and temporal succession of assemblages

Species richness and distribution in the three investigated sediment cores follow the general abundance patterns described by Milzer et al. (2013) from surface sediments in the Trondheimsfjord. Dinocyst assemblages are dominated by *P. dalei* and *O. centrocarpum.* Maximum mean relative abundances of *P.dalei* were found in MC 99-1 in

CPD
9, 4553–4598, 2013

the Seaward basin (67 %) and lowest values in MC 61-1 (50 %) (Fig. 4b). Cysts of *O. centrocarpum* showed highest mean relative abundances in MC 61-1 (34 %) followed by MC 99-1 and MC S4-1 with 25 % (Fig. 4b). Cysts of *S. quanta* and *Brigantedinium spp.* are subordinate in all multi-cores both averaging 5 % in MC 61-1, ca. 1.7 % in MC 99-1, and 3.6 % (*S. quanta*) and 5.1 % (*Brigantedinium spp.*) in MC S4-1. All other species do not exceed > 3 % of the total assemblage.

The recorded species richness and abundances are comparable to the assemblages identified in modern settings of coastal western Norway (Grøsfjeld and Harland, 2001) with the exception of *P. dalei* and *O. centrocrapum*. The reverse dominance of these species in the Trondheimsfjord, with *P. dalei* being the most abundant species, may be explained by the hydrological differences between the well-stratified, brackish and sheltered fjord and the dynamic coastal environment, as already suggested by Grøsfjeld and Harland (2001).

The NMDS classifies the assemblages in the Trondheimsfjord into three groups (stress Shepard plot: 0.06) which are mainly categorized upon the dominant and the subordinate species *P. dalei*, *O. centrocarpum*, *S. quanta* and *Brigantedinium* spp. The classification of samples into one specific group is mainly linked to the varying relative abundance of these species. Statistical analysis with reduced weight on the dominant taxa using log-ratio, or exclusion of the dominant species, did not lead to any reliable grouping (stress Shepard plots: 0.17–0.21) due to the low abundances of the other taxa. The chi-square metric used in CA preserves ecological distances by modeling differences in associations rather than abundances of single species, aiming at extracting groups or data points related to the preferred environmental conditions and possible geographical, stratigraphical or ecological gradients (Hammer et al., 2001). The correspondence analysis identified a total of 16 factors controlling the assemblages with very low eigenvalues (max. eigenvalue: 0.08). The first and the second axis with eigenvalues of 0.08 and 0.02 explain 49 % and 10 % of the variance in the data set, respectively (Fig. 5).

CPD
9, 4553–4598, 2013

Group I is mainly represented in the 1960s and 1970s and therefore only grasped in the sedimentary archives MC 99-1 in the Seaward basin and MC S4-1 at the fjord head (Fig. 5). This group is characterized by a strong dominance of *P. dalei* (60–80 %) over *O. centrocarpum* (lowest recorded abundance within all three cores) (Figs. 5, 7 and 8). All other taxa, mainly represented by *Spiniferites* spp., *S. ramosus*, *S. elongatus* and *Spiniferites* "AW" as well as *A. choane* and *S. quanta* generally add up to < 3 % with very low variability (Figs. 7 and 8). Group II, mostly represented from around 1980–1982, is characterized by slightly decreased abundances of *P. dalei* (48–75 %), which are compensated mainly by increased occurrences of *O. centrocarpum* (19–35 %), *S. quanta* (0.3–7 %), *Brigantedinium spp.* (0.3–9 %), as well as generally minor higher occurrence and variability of all other taxa (Figs. 5–8). Group III is temporally distributed during "transitional periods" between groups I and II. This group is characterized by lowest relative abundances of *P. dalei* and highest occurrences of most other taxa (Fig. 5). This last group explains most of the dinocyst spectra in all three cores during relatively short time intervals of up to 4 yr during the 70's to 80's transition, as well as throughout the final part of the records from ca. 2004 (2000 in MC 61-1) (Figs. 6–8).

According to the core chronologies the resolution of the multi cores is ca. 2 yr cm^{-1}. The chronological framework of the studied cores is related to the classical statistical counting error increasing downcore with maximum deviation of 5 yr (in MC S4-1). Inconsistencies in the order of 2–3 yr in the timing of group changes between the three sediment cores may thus be partly explained by the sampling strategy (1 cm thick homogenized samples) and fall within the error range of dating (higher in bottom parts of the sediment cores). Still, there are few single samples or series of samples which fail to follow this general scheme pointing either to some limitation in the statistical ordination of the data sets, or to local hydrological-sedimentological settings causing irregularities in cyst abundances and diversity. In MC 61-1 the period from 1995 to 2000 differs from the general trend and vary (bi)anually from group I to III (Fig. 6). Around 1995 *P. dalei* shows maximum abundance whereas the other species appear to be less abundant. Minor variation in the relative abundance of *P. dalei* and other taxa

CPD
9, 4553–4598, 2013

with regard to the general temporal trend and associated assemblages determined as group III cause the determination of the years 1998/1999 into group II. The dinocyst distribution in MC 99-1 is generally organized according to the main grouping. Annual and/or biannual periods of relatively enhanced species variability and diversity refer to group III and occur from 1978 to 1980 and around 1996 (Fig. 7). The grouping succession in core MC S4-1 (Fig. 8) displays a series of annual to bi-annual shifts from group I to group II throughout the 70s' to 80's transition as a result of minor changes in dinocyst abundance within years 1976 and 1987.

The three groups and their temporal succession are associated with distinct environmental conditions and potentially with the history of development policies in the Trondheim area and their related impact on the physico-chemical structure and trophic state of the surface waters. The period from the 1960s and the 70s associated with group I, is characterized by a long term negative NAO phase, with lower than normal river discharges into the Seaward Basin and the Middle Fjord, as well as generally negative and positive anomalies in SSTs and SSSs, respectively (Fig. 2). This pattern was interrupted during the early 70s by a short interval of positive NAO pattern and respective changes in the physico-chemical characteristics of the surface waters. The high representation of the cyst assemblages typical of group I within cores MC 99-1 and MC S4-1 during the 60s' and 70s' is supposed to result from the close relationship between NAO phases and SST and SSS changes which is best established before the 1980s'. Low amounts of river discharges from the hinterland and thus reduced supply of nutrients into the fjord impede the production of phytoplankton prey for heterotrophic species from spring to autumn, and explains the scarcity of taxa such as *S. quanta*, *Brigantedinium* spp., *I. minutum* and *L. machaerophorum* in group I (Figs. 7 and 8). Furthermore, low river discharges may also promote the inflow of coastal waters and increase the impact of the tidal surface currents triggering the displacement of cysts into the inner fjord or seaward.

After 1980 the period is mainly represented by group II, and the NAO changed to a long term positive oscillation pattern, resulting in generally higher SSTs, higher than

CPD
9, 4553–4598, 2013

normal river discharges, and lower SSSs (Fig. 2). The temporal distribution of the cyst assemblages referred to group II within the three studied cores is however less straightforward and homogenous than group I before 1980s. This may relate to ill-defined NAO conditions after 1996, leading to rapid fluctuations in SSTs, river discharges and SSSs. Still, the generally higher contributions of heterotrophic species and cysts with a preference for mesotrophic conditions within all cores after 1980 are indicative of enhanced phytoplankton production related to increased nutrient load from rivers and internal mixing. Group III associated with the largest species richness generally occurred throughout the 70s' to 80s' transition as well as after 2000, both periods during which the NAO shifted from one long-term mode to another. Its absence from the most-recent part of core MC 99-1 (Fig. 7) might be related to the regulation of river inputs into the Seaward Basin due to the implementation of hydropower plants in the early-mid 1980s' (Orkla river; L'Abée-Lund et al., 2009). The artificially modified river discharges might account for the heterogenous patterns of discharge anomalies between the rivers Orkla, Gaula and Nidelva (low discharges) and the other major tributaries to the Trondheimsfjord (high discharges) (Fig. 2).

Investigations in southern Norwegian fjords showed that high amounts of nutrients related to industrial activity and effluents caused an increase of the cyst concentration and abundance of heterotrophic species such as *L. machaerophorum* and, in turn, a sharp decrease in the contribution of *P. dalei* (Sætre et al., 1997; Dale et al., 1999a). Regulations to reduce the impact of agricultural and industrial activities on the quality of Trondheimsfjord waters were successfully applied around 1980 (Tangen and Arff, 2003). If eutrophication was one of the important driving forces for the dinocyst production in the Trondheimsfjord during the past 50 yr, this would result into a temporal pattern of the assemblage distribution opposite to the one observed in the present study (Figs. 6–8). We therefore conclude, with the exception of the implementation of hydropower plants, that dinocyst abundance patterns over the last 50 yr were essentially controlled by natural environmental/climatological changes.

CPD
9, 4553–4598, 2013

4.4 Quantitative reconstruction of SSTs, SSSs and PP

The MAT applied for the reconstruction of SSTs and SSSs relate to the best 5 analogues for every multi-core samples with distances below the statistical thresholds for all cores.

Regardless of the site-specific chronological extent and time resolution of the down-core records, reconstructed sea-surface abiotic parameters are generally in good agreement with the modern instrumental data and general temporal variability (Table 2, Fig. 9). Furthermore, reconstructed hydrological values in all cores maintain the overall seasonal temperature and salinity structure of the surface water as recorded at the respective mooring stations (Røberg for MC 61-1 and MC 99-1, and Ytterøy for MC S4-1) with low SSTs and higher SSSs in winter, and high SSTs and slightly lower SSSs in summer. Estimated winter mean SSTs vary between 1.3 °C (MC 99-1) and 3.2 °C (MC 61-1) with minimum and maximum values of −1.6 °C and ca. 8.2 °C for all cores (Table 2, Fig. 9). Reconstructed mean summer SSTs range from 9.2 °C (MC 99-1) to 12.6 °C (MC 61-1) with maximum ranges at site MC 99-1 (ca. 19 °C). Differences between reconstructed and instrumental values are specific to the core locations and the reconstructed (seasonal) hydrographic parameters (Fig. 9). Estimated mean and minimum winter SSTs significantly underestimated at all cores compared to measured winter SSTs (Mann–Whitney test: $p < 0.05$). Maximum estimated winter SSTs in turn, correspond well with the measured winter temperatures at the respective mooring station (p: 0.1–0.5). Reconstructed mean summer SSTs in all cores correspond significantly well with the instrumental summer measurements at the respective mooring stations Røberg and Ytterøy (p: 0.1–0.3). Reconstructed winter SSSs are generally underestimated in all cores with best approximation for the estimated maximum values ($p < 0.05$). Estimated summer SSSs reveal statistically no significant correspondence ($p < 0.05$) with measured data in spite of relatively similar maximum SSSs (Table 2). Qualitatively, most deviations from the instrumental data might be explained by the dominance of *P. dalei* in the fjord area. This species is related to regions characterized

CPD
9, 4553–4598, 2013

by cold and low saline surface layers and seasonal sea-ice cover (e.g. Marret and Zonneveld, 2003; Zonneveld et al., 2013). Furthermore, the production of cysts is season dependent and seasonal SST differences are more extreme in winter than in summer which might explain the generally large underestimation of winter SSTs. An improvement of the estimated values may be achieved by integrating the cyst counts from surface samples in the Trondheimsfjord published in Milzer et al. (2013) in the reference database. However the measured key hydrological parameters in the Trondheimsfjord available today do not properly represent (due to the limited amount of measurement stations) the large heterogeneity of the fjord environment as well as the spatial resolution of the surface sediment database (Milzer et al., 2013). Ultimately, regarding the present study, the dinocyst production in the Trondheimsfjord is to a high extent controlled by the nutrient availability linked to internal mixing and river discharges rather than SSTs and SSSs, which may also account for the uncertainties of the estimated values.

The reconstructed mean annual PP values are lowest at MC 99-1 ($277\,g\,C\,m^{-2}\,yr^{-1}$) and highest at MC 61-1 ($385\,g\,C\,m^{-2}\,yr^{-1}$) (Table 3, Fig. 10). The range between minimum and maximum estimated PP for a given core location is significantly higher in the Seaward Basin and Middle Fjord (ca. 530–$550\,g\,C\,m^{-2}\,yr^{-1}$) than at the fjord entrance (MC 61-1: $400\,g\,C\,m^{-2}\,yr^{-}1$) (Table 3, Fig. 10). In the absence of published datasets on annual rates of primary productivity in the Trondheimsfjord, a proper comparison of estimated vs. measured PP values is not possible. Chlorophyll distributions extracted from moderate resolution images of the spectroradiometer MODIS for the 2002–2005 period translate into an annual primary productivity of 200–$300\,g\,C\,m^{-2}\,yr^{-1}$ along the Norwegian coast (http://daac.gsfc.nasa.gov). This is twice the rate reported by Erga et al. (2005) and Aure et al. (2007) for Norwegian fjords and coastal waters, but corresponds to measured PP in local Scandinavian fjords ranging between 95 and $241\,g\,C\,m^{-2}\,yr^{-1}$ (Grundle et al., 2009 and references therein) as well as to the 150–$300\,g\,C\,m^{-2}\,yr^{-1}$ PP range reported by the UNEP Regional Seas Programme for coastal waters off Norway (Sherman and Hempel, 2008). Our

CPD
9, 4553–4598, 2013

reconstructed mean annual PP in the Trondheimsfjord reveal minimum mean annual PP of ca. 280 $g C m^{-2} yr^{-1}$ in the central Seaward Basin (MC 99-1) and maximum to 385 $g C m^{-2} yr^{-1}$ at the fjord mouth (MC 61-1), and fall within the higher range of most of the above listed measured values for Norwegian fjords and coastal waters.

5 Conclusions

Multivariate analyses of dinocyst census counts in sediment cores of the Trondheimsfjord classify the assemblages into three groups which show a high degree of coherency in terms of temporal succession between the three studied locations. Changes in dinocyst abundances and species diversity mainly reflect multi-annual and decadal-scale changes in NAO pattern and related variability in SSTs, river discharges, SSSs and trophic conditions at the time of cyst production. Significant impact by human activity on the fjord ecological state over the last 50 yr is barely detectable from the investigated micropaleontological successions. Deviations from the NAO-induced pattern of dinocyst assemblage composition between each core site can be mainly explained by local hydrological and topographical features.

Species assemblages in core MC 61-1 at the fjord entrance reveal relatively high species evenness and cyst concentrations. Donwcore changes in species distribution are primarily driven by regional-scale variations in the physico-chemical characteristics of the NCC linked linked to changing continental run-off from southern Scandinavia.

Core site MC 99-1 in the Seaward Basin is located in the flow path of strong tide and bottom water currents, and high river inputs from the local rivers Orkla and Gaula. Both induce inward and seaward displacement of cysts and sediments across the fjord as well as dilution of microfossils by terrigenous sediment. This explains the lowest recorded mean cyst concentrations. However, at this stage we cannot explain the poor species evenness and dominance of *P. dalei* recorded at this location compared with the inner fjord location (MC S4-1).

CPD
9, 4553–4598, 2013

Cyst assemblages at the most inshore site MC S4-1 reflect the relative influence of marine vs. continental climate and associated changes in the physico-chemical surface water characteristics related the prevailing NAO-phase. The core location is strongly influenced by the river Verdalselva. Associated sediment and nutrient loads on one hand trigger cyst production and on the other hand may cause dilution of any fossil remains by terrigenous material.

Reconstructed abiotic and biotic sea-surface parameters are in relatively good agreement with measured time-series SSTs and SSSs in the Trondheimsfjord as well as with datasets from coastal Norway and other Scandinavian fjords (mean annual PPs). Best estimates are generally achieved for summer SST and SSS conditions constraining both the site selection as well as the chosen parameters for future quantitative Holocene climate and hydrological reconstructions.

Acknowledgements. This work is a contribution to the CASE Initial Training Network funded by the European Community's 7th Framework Programme FP7 2007/2013, Marie-Curie Actions, under Grant Agreement No. 238111. (http://caseitn.epoc.u-bordeaux1.fr/). Temperature and salinity datasets from the fjord hydrological mooring stations are provided by the Trondheim Biological Station of the Norwegian University of Science and Technology. We gratefully acknowledge Bendik Eithun Halgunset from Sør-Trøndelag Fylkeskommune, Viggo Finset from TrønderEnergi Kraft AS, as well as Arne Jørgen Kjøsnes and Eva Klausen from Norwegian Water Resources and Energy Directorate for their cooperation, helpful suggestions and data access. Anne de Vernal (GEOTOP, UQAM) is gratefully acknowledged for her support, helpful suggestions and reference data.

The publication of this article is financed by CNRS-INSU.

CPD
9, 4553–4598, 2013

References

Appleby, P. G.: Chronostratigraphic techniques in recent sediments, in: Tracking Environmental Change Using Lake Sediments, volume 1: Basin Analysis, Coring, and Chronological Techniques, edited by: Last, W. M. and Smol, J. P., Kluwer Academic Publishers, Dordrecht, the Netherlands, 2001.

Aure, J., Strand, Ø., Erga, S., and Strohmeier, T.: Primary production enhancement by artificial upwelling in a western Norwegian fjord, Mar. Ecol.-Prog. Ser., 352, 39–52, doi:10.3354/meps07139, 2007.

Bigler, C. and Wunder, J.: Statistische Datenanalyse mit R?: Eine Einführung für Umweltwissenschaftler, Gebirgswaldökologie (D-FOWI), Eidgenössische Technische Hochschule (ETH) Zürich, Switzerland, 1–39, 2003.

Blindheim, J., Borovkov, V., Hansen, B., Malmberg, S.-A., Turrell, W. R., and Østerhus, S.: Upper layer cooling and freshening in the Norwegian Sea in relation to atmospheric forcing, Deep-Sea Res. Pt. I, 47, 655–680, doi:10.1016/S0967-0637(99)00070-9, 2000.

Bøe, R., Rise, L., Blikra, L. H., Longva, O., and Eide, A.: Holocene mass-movement processes in Trondheimsfjorden, Central Norway, Norw. J. Geol., 83, 3–22, 2003.

Dale, B.: Cyst formation, sedimentation and preservation: factors affecting dinoflagellate assemblages in recent sediments from Trondheimsfjord, Norway, Rev. Palaeobot. Palynol., 22, 39–60, 1976.

Dale, B.: Marine dinoflagellate cysts as indicators of eutrophication and industrial pollution: a discussion, The Sci. Total. Environ., 264, 235–240, 2001.

Dale, B., Thorsen, T. A., and Fjellsa, A.: Dinoflagellate cysts as indicators of cultural eutrophication in the Oslofjord, Norway, Estuar. Coast. Shelf S., 48, 371–382, doi:10.1006/ecss.1999.0427, 1999a.

Dale, T., Rey, F., and Heimdal, B. R.: Seasonal development of phytoplankton at a high latitude oceanic site, Sarsia, 84, 419–435, 1999b.

Dale, B., Dale, A. L., and Jansen, J. H. F.: Dinoflagellate cysts as environmental indicators in surface sediments from the Congo deep-sea fan and adjacent regions, Palaeogeogr. Palaeocl., 185, 309–338, 2002.

de Vernal, A. and Marret, F.: Organic-walled dinoflagellate cysts: tracers of sea-surface conditions, Mar. Geol., 1, 371–408, doi:10.1016/S1572-5480(07)01014-7, 2007.

CPD
9, 4553–4598, 2013

de Vernal, A., Rochon, A., Hillaire-Marcel, C., Turon, J. L., and Guiot, J.: Quantitative reconstruction of sea-surface conditions, seasonal extent of sea-ice cover and meltwater discharges in high latitude marine environments from dinoflagellate cyst assemblages, Nato. Asi. Series, I12, 611–621, 1993.

de Vernal, A., Henry, M., and Bilodeau, G.: Techniques de Préparation et d'Analyse en Micropaleontologie, Le Cahiers du GEOTOP, 3, Université du Québec à Montréal, Canada, 1996.

de Vernal, A., Hillaire-Marcel, C., Turon, J.-L., and Matthiessen, J.: Reconstruction of sea-surface temperature, salinity, and sea-ice cover in the northern North Atlantic during the last glacial maximum based on dinocyst assemblages, Can. J. Earth Sci., 37, 725–750, doi:10.1139/e99-091, 2000.

de Vernal, A., Henry, M., Matthiessen, J., Mudie, P. J., Rochon, A., Boessenkool, K. P., Eynaud, F., Grøsfjeld, K., Guiot, J., Hamel, D., Harland, R., Head, M. J., Kunz-Pirrung, M., Levac, E., Loucheur, V., Peyron, O., Pospelova, V., Radi, T., Turon, J.-L., and Voronina, E.: Dinoflagellate cyst assemblages as tracers of sea-surface conditions in the northern North Atlantic, Arctic and sub-Arctic seas: the new $n = 677$ data base and its application for quantitative palaeoceanographic reconstruction, J. Quaternary Sci., 16, 681–698, doi:10.1002/jqs.659, 2001.

de Vernal, A., Eynaud, F., Henry, M., Hillaire-Marcel, C., Londeix, L., Mangin, S., Matthiessen, J., Marret, F., Radi, T., Rochon, A., Solignac, S., and Turon, J.-L.: Reconstruction of sea-surface conditions at middle to high latitudes of the Northern Hemisphere during the Last Glacial Maximum (LGM) based on dinoflagellate cyst assemblages, Quaternary Sci. Rev., 24, 897–924, doi:10.1016/j.quascirev.2004.06.014, 2005.

Devillers, R. and de Vernal, A.: Distribution of dinoflagellate cysts in surface sediments of the northern North Atlantic in relation to nutrient content and productivity in surface waters, Mar. Geol., 166, 103–124, doi:10.1016/S0025-3227(00)00007-4, 2000.

Durantou, L., Rochon, A., Ledu, D., Massé, G., Schmidt, S., and Babin, M.: Quantitative reconstruction of sea-surface conditions over the last 150 yr in the Beaufort Sea based on dinoflagellate cyst assemblages: the role of large-scale atmospheric circulation patterns, Biogeosciences, 9, 5391–5406, doi:10.5194/bg-9-5391-2012, 2012.

Ellingsen, I. H.: Internal tides and the spread of river plumes in the Trondheimfjord, Norwegian University of Science and Technology (NTNU), Trondheim, 1–174, 2004.

CPD
9, 4553–4598, 2013

Erga, S. R., Aursland, K., Frette, Ø., Hamre, B., Lotsberg, J. K., Stamnes, J. J., Aure, J., Rey, F., and Stamnes, K.: UV transmission in Norwegian marine waters: controlling factors and possible effects on primary production and vertical distribution of phytoplankton, Mar Ecol. Prog. Ser., 305, 79–100, doi:10.3354/meps305079, 2005.

Grøsfjeld, K. and Harland, R.: Distribution of modern dinoflagellate cysts from inshore areas along the coast of southern Norway, J. Quaternary Sci., 16, 651–659, doi:10.1002/jqs.653, 2001.

Grøsfjeld, K., Larsen, E., Sejrup, H. P., De Vernal, A., Flatebø, T., Vestbø, M., Haflidason, H., and Aarseth, I.: Dinoflagellate cysts reflecting surface-water conditions in Voldafjorden, western Norway during the last 11 300 years, Boreas, 28, 403–415, 1999.

Grundle, D. S., Timothy, D. A., and Varela, D. E.: Variations of phytoplankton productivity and biomass over an annual cycle in Saanich Inlet, a British Columbia fjord, Cont. Shelf Res., 29, 2257–2269, doi:10.1016/j.csr.2009.08.013, 2009.

Guiot, J. and de Vernal, A.: Transfer functions: methods for quantitative paleoceanography based on microfossils, in: Proxies in Late Cenozoic Paleoceanography, vol. 1, edited by: Hillaire-Marcel, C. and de Vernal, A., Elsevier, 523–563, doi:10.1016/S1572-5480(07)01018-4, 2007.

Hammer, Ø., Harper, D. A. T., and Ryan, P. D.: Paleontological Statistics software package for education and data analysis, Paleontologia Electronica, 4, 9 pp., version 2.15 (April 2012), available at: http://www.folk.uio.no/ohammer/past, 2001.

Harland, R.: Distribution maps of recent dinoflagellate cysts in bottom sediments from the North Atlantic Ocean and adjacent seas, Paleontology, 26, 321–387, 1983.

Harland, R., Nordberg, K., and Filipsson, H. L.: A high-resolution dinoflagellate cyst record from latest Holocene sediments in Koljö Fjord, Sweden, Rev. Palaeobot. Palynol., 128, 119–141, doi:10.1016/S0034-6667(03)00116-7, 2004.

Harland, R., Nordberg, K., and Filipsson, H. L.: Dinoflagellate cysts and hydrographical change in Gullmar Fjord, west coast of Sweden, Sci. Total Environ., 355, 204–231, doi:10.1016/j.scitotenv.2005.02.030, 2006.

Head, M. J., Harland, R., and Matthiessen, J.: Cold marine indicators of the late Quaternary: the new dinoflagellate cyst genus Islandinium and related morphotypes, J. Quaternary Sci., 16, 621–636, doi:10.1002/jqs.657, 2001.

CPD
9, 4553–4598, 2013

Head, M. J., Lewis, J., and de Vernal, A.: The cyst of the calcareous dinoflagellate Scrippsiella trifida; resolving the fossil record of its organic wall with that of Alexandrium tamarense, J. Paleontol., 80, 1–18, 2006.
Holland, S. M.: Non-Metric Multidimensional Scaling (MDS) (May), available at: strata.uga.edu/software/pdf/mdsTutorial.pdf (last access: May 2013), 2008.
Howe, J. A., Austin, W. E. N., Forwick, M., and Paetzel, M. (Eds.): Fjord Systems and Archives, Geological Society, Special Publications, London, 2010.
Hurrell, J. W.: Decadal trends in the North Atlantic Oscillation: regional temperatures and precipitation, Science, 269, 676–679, 1995.
Hurrell, J. W. and van Loon, H.: Decadal variations in climate associated with the North Atlantic Oscillation, in: Climatic Change, Vol. 36, Kluwer Academic Publishers, Dordrecht, the Netherlands, 301–326, 1997.
Jacobson, P.: Physical oceanography of the Trondheimsfjord, Geophysi. Astro. Fluid, 26, 3–26, 1983.
Kirchner, G.: ^{210}Pb as a tool for establishing sediment chronologies: examples of potentials and limitations of conventional dating models, J. Environ. Radioactiv., 102, 490–494, doi:10.1016/j.jenvrad.2010.11.010, 2011.
L'Abée-Lund, J. H., Eie, J. A., Faugli, P. E., Haugland, S., Hvidsten, N. A., Jensen, A. J., Melvold, K., Pettersen, V., and Saltveit, S. J.: Rivers in boreal uplands, in: Rivers of Europe, edited by: Tockner, K., Robinson, C. T., and Uehlinger, U., Academic Press, Elsevier, 699 pp., 2009.
Loeng, H. and Drinkwater, K.: An overview of the ecosystems of the Barents and Norwegian Seas and their response to climate variability, Deep Sea Res. Pt. II, 54, 2478–2500, doi:10.1016/j.dsr2.2007.08.013, 2007.
Marret, F. and Zonneveld, K.: Atlas of modern organic-walled dinoflagellate cyst distribution, Rev. Palaeobot. Palynol., 125, 1–200, doi:10.1016/S0034-6667(02)00229-4, 2003.
Marret, F., Eiríksson, J., Knudsen, K. L., Turon, J.-L., and Scourse, J. D.: Distribution of dinoflagellate cyst assemblages in surface sediments from the northern and western shelf of Iceland, Rev. Palaeobot. Palynol., 128, 35–53, doi:10.1016/S0034-6667(03)00111-8, 2004.
Matthiessen, J.: Distribution patterns of dinoflagellate cysts and other organic-walled microfossils in recent Norwegian-Greenland Sea sediments, Mar. Micropaleontol., 24, 307–334, doi:10.1016/0377-8398(94)00016-G, 1995.

CPD
9, 4553–4598, 2013

McMinn, A.: Recent dinoflagellate cysts from estuaries on the central coast of New South Wales, Australia, Micropaleontology, 37, 269–287, 1991.
Milzer, G., Giraudeau, J., Faust, J., Knies, J., Eynaud, F., and Rühlemann, C.: Spatial distribution of benthic foraminiferal stable isotopes and dinocyst assemblages in surface sediments of the Trondheimsfjord, central Norway, Biogeosciences, 10, 4433–4448, doi:10.5194/bg-10-4433-2013, 2013.
Nehring, S., Kiel, D. U., Weg, D., and Kiel, D: Dinoflagellate resting cysts in recent sediments of tide western Baltic as indicators for the occurrence of "non-indigenous" species in the water column, Bransonic, 52, 79–85, 1997.
Ottersen, G., Planque, B., Belgrano, A., Post, E., Reid, P., and Stenseth, N.: Ecological effects of the North Atlantic Oscillation, Oecologia, 128, 1–14, doi:10.1007/s004420100655, 2001.
Parke, M. and Dixon, P. S.: Revised check-list of British marine algae, J. Mar. Biol. Assoc. UK, 44, 499–542, 1964.
Penaud, A., Eynaud, F., Turon, J. L., Zaragosi, S., Marret, F., and Bourillet, J. F.: Interglacial variability (MIS 5 and MIS 7) and dinoflagellate cyst assemblages in the Bay of Biscay (North Atlantic), Mar. Micropal., 68, 136–155, doi:10.1016/j.marmicro.2008.01.007, 2008.
Pettersson, L.-E.: Totalavløpet fra Norges vassdrag 1900–2010 (Rapport nr 39-2012), Oslo, ISBN: 978-82-410-0827-6, 2012.
Pospelova, V., Esenkulova, S., Johannessen, S. C., O'Brien, M. C., and Macdonald, R. W.: Organic-walled dinoflagellate cyst production, composition and flux from 1996 to 1998 in the central Strait of Georgia (BC, Canada): a sediment trap study, Mar. Micropaleontol., 75, 17–37, doi:10.1016/j.marmicro.2010.02.003, 2010.
Price, A. M. and Pospelova, V.: High-resolution sediment trap study of organic-walled dinoflagellate cyst production and biogenic silica flux in Saanich Inlet (BC, Canada), Mar. Micropaleontol., 80, 18–43, doi:10.1016/j.marmicro.2011.03.003, 2011
Radi, T. and de Vernal, A.: Dinocyst distribution in surface sediments from the northeastern Pacific margin (40–60° N) in relation to hydrographic conditions, productivity and upwelling, Rev. Palaeobot. Palynol., 128, 169–193, doi:10.1016/S0034-6667(03)00118-0, 2004.
Radi, T. and de Vernal, A.: Dinocysts as proxy of primary productivity in mid–high latitudes of the Northern Hemisphere, Mar. Micropaleontol., 68, 84–114, doi:10.1016/j.marmicro.2008.01.012, 2008.

CPD
9, 4553–4598, 2013

Radi, T., Pospelova, V., de Vernal, A., and Vaughn, B., J.: Dinoflagellate cysts as indicators of water quality and productivity in British Columbia estuarine environments, Mar. Micropaleontol., 62, 269–297, doi:10.1016/j.marmicro.2006.09.002, 2007.
Riding, J. B. and Kyffin-Hughes, J. E.: A review of the laboratory preparation of palynomorphs with a description of an effective non-acid technique, Rev. Bras. Paleontol., 7, 13–44, 2004.
Robbins, J. A. and Edgington, D. N.: Determination of recent sedimentation rates in Lake Michigan using Pb-210 ad CS-137, Geochim. Cosmochim. Ac., 39, 285–304, 1975.
Rochon, A., De Vernal, A., Turon, J.-L., Matthiessen, J., and Head, M. J.: Distribution of recent dinoflagellate cysts in surface sediments from the North Atlantic Ocean and adjacent seas in relation to sea-surface parameters, Am. Assoc. Strat. Palynol., 35, 1–146, doi:10.1016/0377-8398(94)00016-G, 1999.
Sætre, M. M. L., Dale, B., Abdullahb, M. I., and Sætre, G. P.: Dinoflagellate cysts as potential indicators of industrial pollution in a Norwegian fjord, Mar. Environ. Res., 44, 167–189, 1997.
Sætre, R.: Features of the central Norwegian shelf circulation, Cont. Shelf Res., 19, 1809–1831, 1999.
Sætre, R. (Ed.): Norwegian Coastal Current, Tapir Academic Press, 2007.
Sakshaug, E. and Myklestad, S.: Studies on the phytoplankton ecology of the Trondheimsfjord. III Dynamics of phytoplankton blooms in relation to environmental factors, bioassy experiments and parameters for the physiological state of the populations, J. Exp. Mar. Biol. Ecol., 11, 157–188, 1973.
Schmidt, S., Howa, H., Diallo, A., Cremer, M., Duros, P., Fontanier, C., Deflandre, B., Metzger, E., and Mulder, T.: Recent sediment transport and deposition in the Cap-Ferret Canyon, South-East margin of Bay of Biscay, Deep-Sea Res. Pt. II, online first, doi:10.1016/j.dsr2.2013.06.004, 2013.
Sherman, K. and Hempel, G.: The UNEP Large Marine Ecosystem Report: a perspective on changing conditions in LMEs of the world's Regional Seas, United Nations Environment Programme, Nairobi, Kenya, 2008.
Smayda, T. J. and Reynolds, C. S.: Strategies of marine dinoflagellate survival and some rules of assembly, J. Sea Res., 49, 95–106, doi:10.1016/S1385-1101(02)00219-8, 2003.
Sorrel, P., Popescu, S.-M., Head, M. J., Suc, J. P., Klotz, S., and Oberhänsli, H.: Hydrographic development of the Aral Sea during the last 2000 years based on a quantitative analysis of dinoflagellate cysts, Palaeogeogr. Palaeocl., 234, 304–327, doi:10.1016/j.palaeo.2005.10.012, 2006.

CPD
9, 4553–4598, 2013

Stockmarr, J.: Tablets with spores used in absolute pollen analysis, Pollen Spores, 8, 615–621, 1971.
Strømgren, T.: Zooplankton and Hydrography in Trondheimsfjorden on the west coast of Norway, Royal Norwegian Soc. Sci. Lett. Mus., 51–60, 1–38, doi:10.1016/0024-3841(84)90026-3, 1974.
Tangen, K. and Arff, J.: Høvringen wastewater plant and the environmental quality of the Trondheimfjord (OCN R-23027), Trondheim (Norway), 2003.
van der Klooster, E., van Egmond, F. M., and Sonneveld, M. P. W.: Mapping soil clay contents in Dutch marine districts using gamma-ray spectrometry, Eur. J. Sci., 62, 743–753, doi:10.1111/j.1365-2389.2011.01381.x, 2011.
van Nieuwenhove, N., Bauch, H., and Matthiessen, J.: Last interglacial surface water conditions in the eastern Nordic Seas inferred from dinocyst and foraminiferal assemblages, Mar. Micropaleontol., 66, 247–263, doi:10.1016/j.marmicro.2007.10.004, 2008.
Visbeck, M., Chassignet, E. P., Curry, R., Dickson, B., and Krahmann, G.: The ocean's response to North Atlantic Oscillation variability, in: The North Atlantic Oscillation: Climatic Significance and Environmental Impact, edited by: Hurrell, J. W., Washington D. C., 113–145, 2003.
von Detten, P., Faude, O., and Meyer, T.: Leitfaden zur statistischen Auswertung von empirischen Studien, Institut für Sportmedizin, Universität Paderborn, Paderborn, Germany, 1–44, 2008.
Wall, D. and Dale, B.: The resting cysts of modern marine dinoflagellates and their paleontological significance, Rev. Palaeobot. Palynol., 2, 349–354, 1967.
Zaragosi, S., Eynaud, F., Pujol, C., Auffret, G. A., Turon, J.-L., and Garlan, T.: Initiation of the European deglaciation as recorded in the northwestern Bay of Biscay slope environments (Meriadzek Terrace and Trevelyan Escarpment): a multi-proxy approach, Earth Planet. Sc. Lett., 188, 493–507, 2001.
Zonneveld, K. A. F., Versteegh, G. J. M., and De Lange, G. J.: Preservation of organic-walled dinoflagellate cysts in different oxygen regimes: a 10 000 year natural experiment, Mar. Micropaleontol., 393–405, 1997.
Zonneveld, K. A. F., Versteegh, G. J. M., and De Lange, G. J.: Palaeoproductivity and post-depositional aerobic organic matter decay reflected by dinoflagellate cyst assemblages of the Eastern Mediterranean S1 sapropel ABC26, Mar. Geol., 172, 181–195, 2001.

CPD
9, 4553–4598, 2013

Zonneveld, K. A. F., Versteegh, G., and Kodrans-Nsiah, M.: Preservation and organic chemistry of Late Cenozoic organic-walled dinoflagellate cysts: a review, Mar. Micropaleontol., 68, 179–197, doi:10.1016/j.marmicro.2008.01.015, 2008.

Zonneveld, K. A. F., Marret, F., Versteegh, G. J. M., Bogus, K., Bonnet, S., Bouimetarhan, I., Crouch, E., De Vernal, A., Elshanawany, R., Edwards, L., Esper, O., Forke, S., Grøsfjeld, K., Henry, M., Holzwarth, U., Kielt, J.-F., Kim, S.-Y., Ladouceur, S., Ledu, D., Chen, L., Limoges, A., Londeix, L., Lu, S.-H., Mahmoud, M. S., Marino, G., Matsouka, K., Matthiessen, J., Mildenhal, D. C., Mudie, P., Neil, H. L., Pospelova, V., Qi, Y., Radi, T., Richerol, T., Rochon, A., Sangiorgi, F., Solignac, S., Turon, J.-L., Verleye, T., Wang, Y., Wang, Z., and Young, M.: Atlas of modern dinoflagellate cyst distribution based on 2405 data points, Rev. Palaeobot. Palynol., 191, 1–197, doi:10.1016/j.revpalbo.2012.08.003, 2013.

CPD
9, 4553–4598, 2013

Table 1. Site locations, water depths and core lengths.

Multi core	Location	Longitude [degrees_east]	Latitude [degrees_north]	Water depth [m]	Core length (cm)
MC 61-1	Stjørnfjord	9°86′ E	63°71′ N	225	12
MC 99-1	Seaward Basin	10°19′ E	63°48′ N	504	24
MC S4-1	Middle Fjord	10°98′ E	63°73′ N	420	40

CPD
9, 4553–4598, 2013

Table 2. Descriptive statistics of measured and estimated winter and summer SSTs and SSSs with a 95 % confidence level. Standard error for the mean values and standard deviation for the mode values are in brackets. Instrumental measurements were monitored at 10 m water depths at the mooring stations Røberg and Ytterøy; estimated SSTs and SSSs are denoted by the core name and compared with the surface water parameters of the nearest mooring station: MC 61-1 and MC 99-1 with Røberg and MC S4-1 with Ytterøy.

	SST Winter					SST Summer				
	Røberg	MC 61-1	MC 99-1	Ytterøy	MC S4-1	Røberg	MC 61-1	MC 99-1	Ytterøy	MC S4-1
Mean	4.7 (0.1)	3.2 (0.5)	1.3 (0.4)	4.2 (0.1)	1.9 (0.3)	11.0 (0.2)	12.6 (0.7)	9.2 (0.7)	10.4 (0.2)	11.3 (0.5)
Median	4.8	3.2	0.7	4.2	1.7	11.0	12.6	8.9	10.4	10.6
Mode	3.5 (1.0)	1.5 (3.1)	−1.5 (3.0)	3.7 (1.0)	4.8 (2.9)	11.3 (1.9)	17.7 (4.0)	17.7 (5.5)	11.1 (2.0)	17.7 (4.7)
Variance	1.1	9.7	9.0	0.9	8.4	3.7	16.1	30.7	3.9	21.8
Kurstosis	−0.2	−0.8	−0.2	0.1	−0.8	−0.2	−1.5	−0.8	−0.7	−1.0
Skewness	0.1	0.1	0.8	0.4	0.4	−0.1	0.1	0.1	0.0	0.0
Range	5.1	9.8	10.0	4.9	10.0	10.0	10.8	19.0	8.5	17.4
Minimum	2.6	−1.6	−1.8	2.1	−1.8	5.9	6.8	−1.3	6.2	0.3
Maximum	7.7	8.2	8.2	7.0	8.2	15.9	17.7	17.7	14.7	17.7
	SSS Winter					SSS Summer				
	Røberg	MC 61-1	MC 99-1	Ytterøy	MC S4-1	Røberg	MC 61-1	MC 99-1	Ytterøy	MC S4-1
Mean	32.5 (0.1)	29.9 (0.6)	30.3 (0.4)	32.0 (0.1)	29.9 (0.4)	31.1 (0.1)	27.3 (0.9)	27.6 (0.6)	30.6 (0.1)	27.2 (0.5)
Median	32.7	30.7	31.0	32.1	30.7	31.2	29.0	28.4	30.8	28.5
Mode	32.0 (0.9)	25.4 (3.5)	25.4 (3.2)	31.8 (1.1)	25.4 (3.3)	31.2 (1.4)	20.4 (5.2)	20.4 (4.8)	32.0 (1.5)	20.4 (5.1)
Variance	0.9	12.0	10.2	1.2	11.1	2.0	27.5	23.2	2.2	25.9
Kurstosis	1.1	−1.5	−1.1	0.3	−1.4	4.0	−1.4	−1.0	1.3	−1.4
Skewness	−1.1	−0.2	−0.4	−0.7	−0.3	−1.2	−0.3	−0.3	−0.9	−0.3
Range	4.6	9.5	9.4	5.7	9.8	9.5	14.4	14.3	8.7	14.7
Minimum	29.5	25.4	25.4	28.2	25.4	24.1	20.4	20.4	24.7	20.4
Maximum	34.1	34.8	34.8	34.0	35.1	33.6	34.7	34.6	33.4	35.0

CPD
9, 4553–4598, 2013

Table 3. Descriptive statistics of MAT reconstructions of annual primary productivity (confidence level of 95 %); standard error for the mean values and the standard deviation for the mode values are in brackets.

	Productivity		
	MC 61-1	MC 99-1	MC S4-1
Mean	384.7 (24.2)	276.7 (19.7)	326.3 (15.7)
Median	375.4	235.1	297.0
Mode	567.0 (145.1)	567.0 (167.4)	567.0 (149.4)
Kurstosis	−1.6	−0.7	−0.9
Skewness	0.1	0.6	0.4
Range	406.3	551.0	531.7
Minimum	160.7	16.1	35.3
Maximum	567.0	567.0	567.0

CPD
9, 4553–4598, 2013

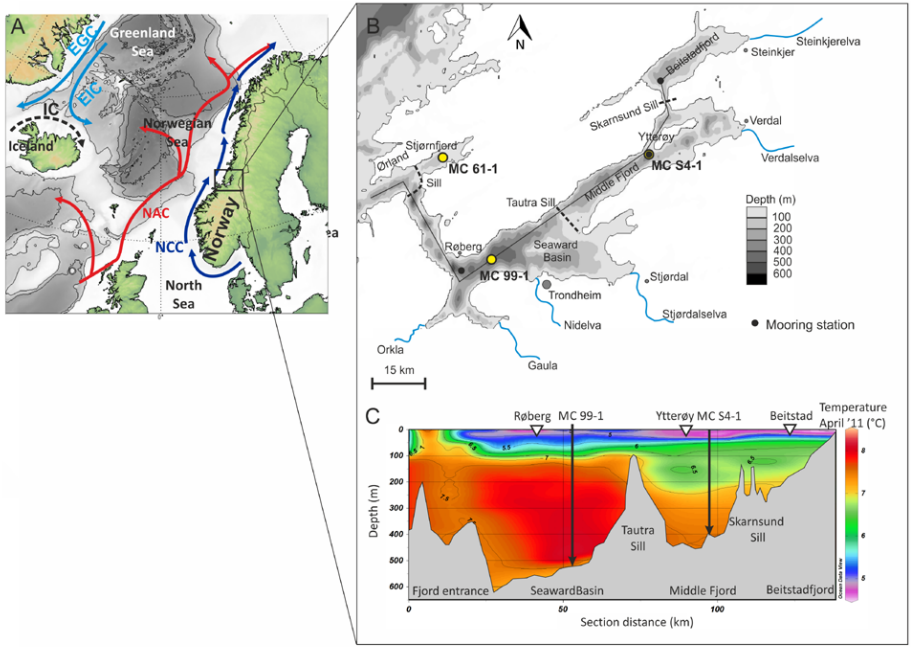

Fig. 1. (A) Surface circulation in the North Atlantic region; **(B)** bathymetric map of the Trondheimsfjord modified from Milzer et al. (2013). Yellow dots indicate the core locations, black dots the fixed mooring stations Røberg, Ytterøy and Beitstad referred to in the text; **(C)** temperature structure of the water column along the fjord axis in April 2011 (modified from Milzer et al., 2013); locations of MC99-1 and MC S4-1 (black arrows) and the mooring stations Røberg, Ytterøy and Beitstad (white triangles) are also indicated along the fjord axis. The location of MC 61-1 is outside the cross section.

CPD
9, 4553–4598, 2013

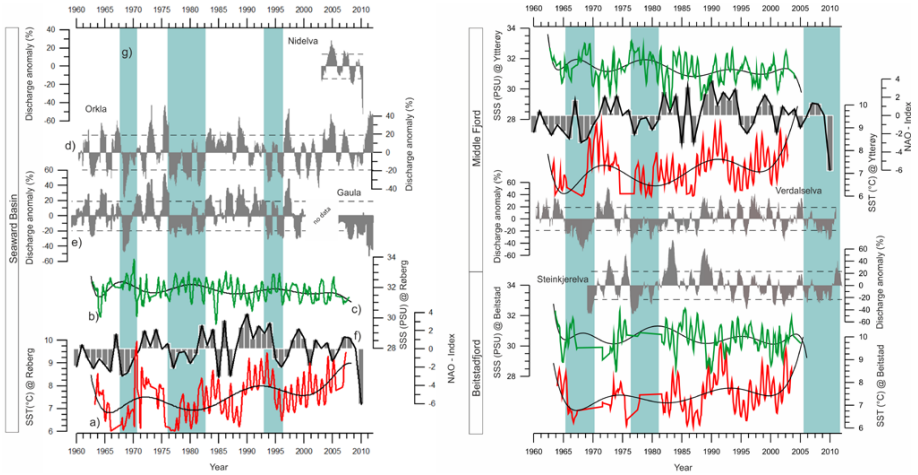

Fig. 2. Hydrological and climatic data: Red lines **(a)** illustrate the 15 pt. running average of annual SSTs and green lines **(b)** the 7 pt. running average of SSSs monitored at the mooring stations Røberg, Ytterøy and Beitstad at 10 m water depth from 1963 to 2005; black lines **(c)** represent the associated 7 and 10 order polynomial functions of SST and SSS, respectively; grey shaded graphs **(d)** display the annual running average of river discharge anomalies ($m^3\ yr^{-1}$ in % below/above the 50 yr mean value (data from Norwegian Water Resources and Energy Directorate (NVE): www.nve.no) with **(e)** grey dashed lines: standard deviation of river discharges in % during the past 50 yr; grey black-framed columns **(f)** show the NAO – index (Hurrel, 1995); blue columns **(g)** mark negative anomalies of river discharge.

CPD
9, 4553–4598, 2013

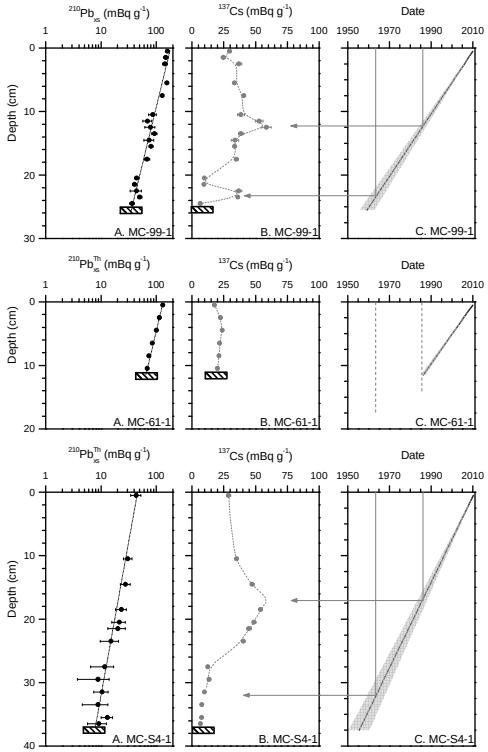

Fig. 3. Core chronology of MC 61-1 (center) at the fjord entrance, MC 99-1 (top) in the Seaward Basin and MC S4-1 (bottom) in the Middle Fjord showing **(A)** $^{210}Pb_{xs}$ or $^{210}Pb^{Th}_{xs}$ (i.e. $^{210}Pb_{xs}$ normalized to ^{232}Th, explanation in the text) profiles, **(B)** ^{137}Cs profiles (except for MC 61-1, explanation in the text) and **(C)** calculated ages based on the CF : CS model. The arrows indicate the expected position of the ^{137}Cs peaks related to maximum weapon test atmospheric fallout and Chernobyl accident according to the chronology based on $^{210}Pb_{xs}$.

CPD
9, 4553–4598, 2013

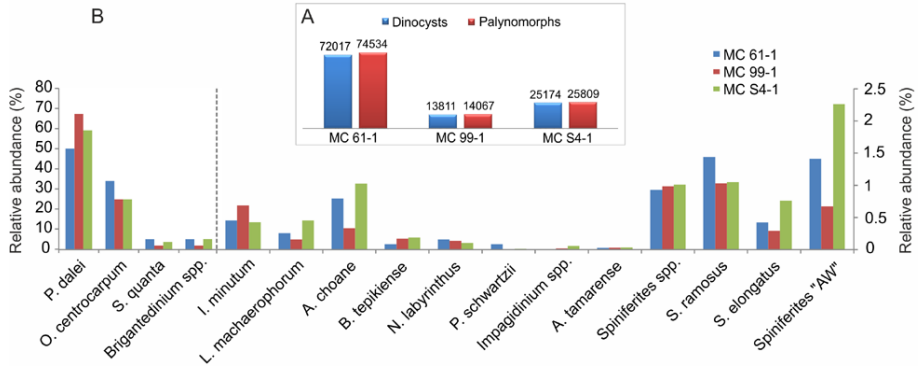

Fig. 4. (A) mean absolute (number of cysts cm^{-3}) and **(B)** relative (%) cyst abundances in the Trondheimsfjord; grey dashed line divides the species with regard to the respective y-axis: species on the left side refer to the left axis (high relative abundances), species on the right side to the right axis (low abundances).

CPD
9, 4553–4598, 2013

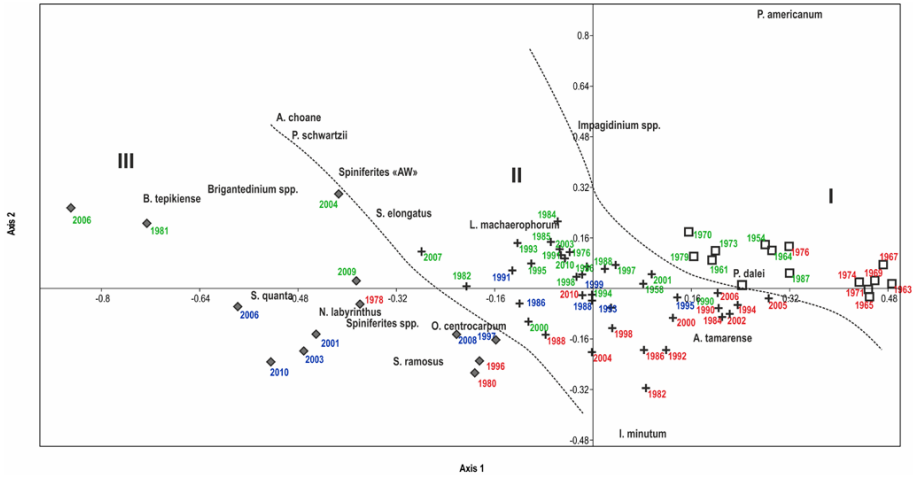

Fig. 5. Correspondence analysis based on relative cyst abundances of all cores combined as one data set, and groups determined by the NMDS. Hollow squares display the years associated with group I, crosses refer to group II and grey shaded diamonds to group III. The species are ordinated by the CA according to coexistence and variability of cysts. The coloured numbers are organized by sediment cores: MC 61-1: blue; MC 99-1: red and MC S4-1: green; samples belonging to group I are placed on the positive axis 1 in correspondence with the dominance of *P. dalei*, minimum abundances or absence of other taxa; samples categorized into group II are placed in the center of the CA, and representatives of group III on the far negative axis 1.

CPD
9, 4553–4598, 2013

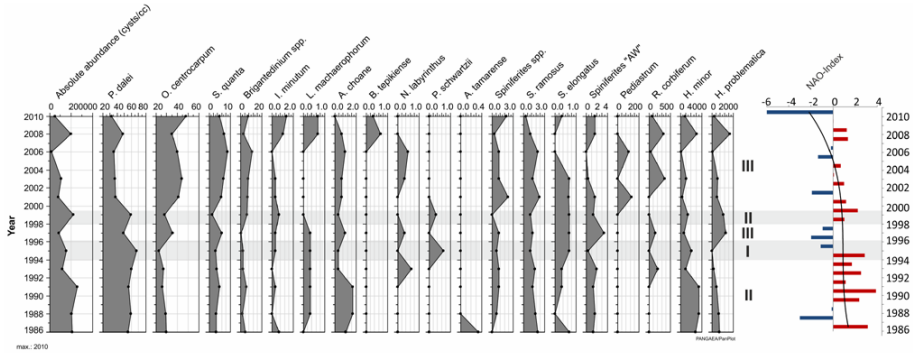

Fig. 6. Cyst assemblages in MC 61-1 and associated groups according to NMDS; cyst concentrations and Chlorophycean and Prasinophyceae algae are given in nb cc-1, relative dinocyst abundances are given in %; the NAO index is shown to the right (Hurrel, 1995).

CPD
9, 4553–4598, 2013

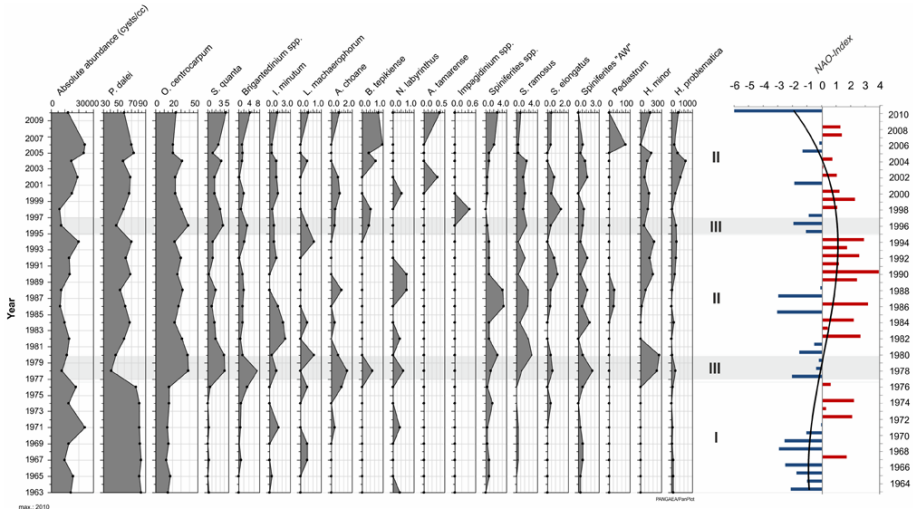

Fig. 7. Cyst assemblages in MC 99-1 and associated groups according to NMDS; cyst concentration and Chlorophycean and Prasinophyceae algae are given in nb cc-1, relative dinocyst abundances are given in %; the NAO index is shown to the right (Hurrel, 1995).

CPD
9, 4553–4598, 2013

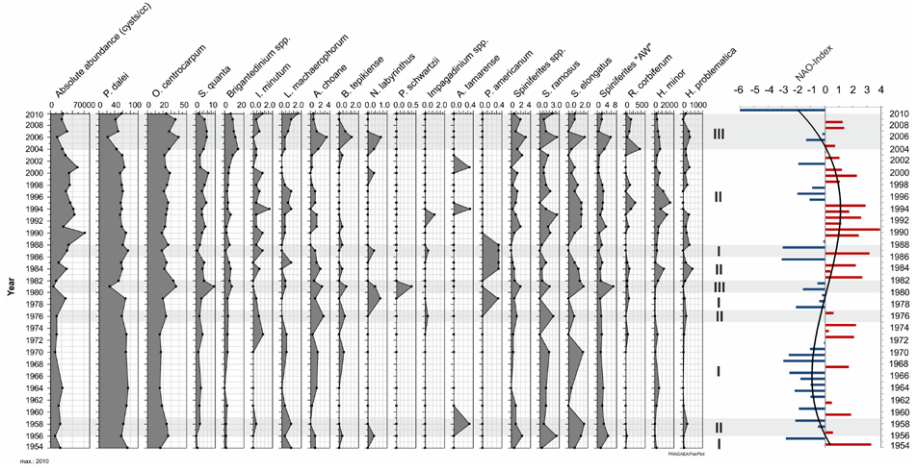

Fig. 8. Cyst assemblages in MC S4-1 and associated groups according to NMDS; cyst concentrations and Chlorophycean and Prasinophyceae algae are given in nb cm^{-3}, relative dinocyst abundances are given in %; the NAO index is shown to the right (Hurrel, 1995).

CPD
9, 4553–4598, 2013

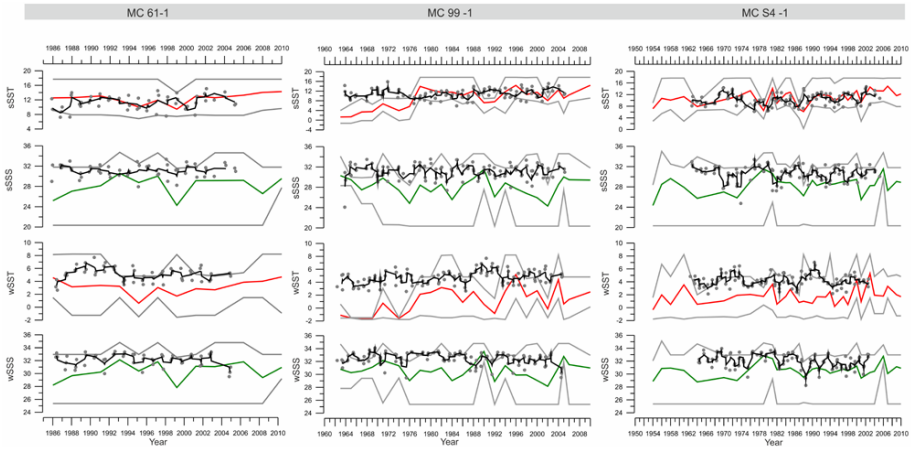

Fig. 9. Winter and summer SST and SSS reconstructions based on cyst assemblages at every core site; red line: mean SST; green: mean SSS; grey lines: associated min. and max. values calculated from the set of the 5 selected analogues; grey dots: instrumental temperatures and salinities measured at the respective mooring station, Røberg for MC 61-1 and MC 99-1 and Ytterøy for MC S4-1; black lines are the three point running average of the instrumental temperatures and salinities.

CPD
9, 4553–4598, 2013

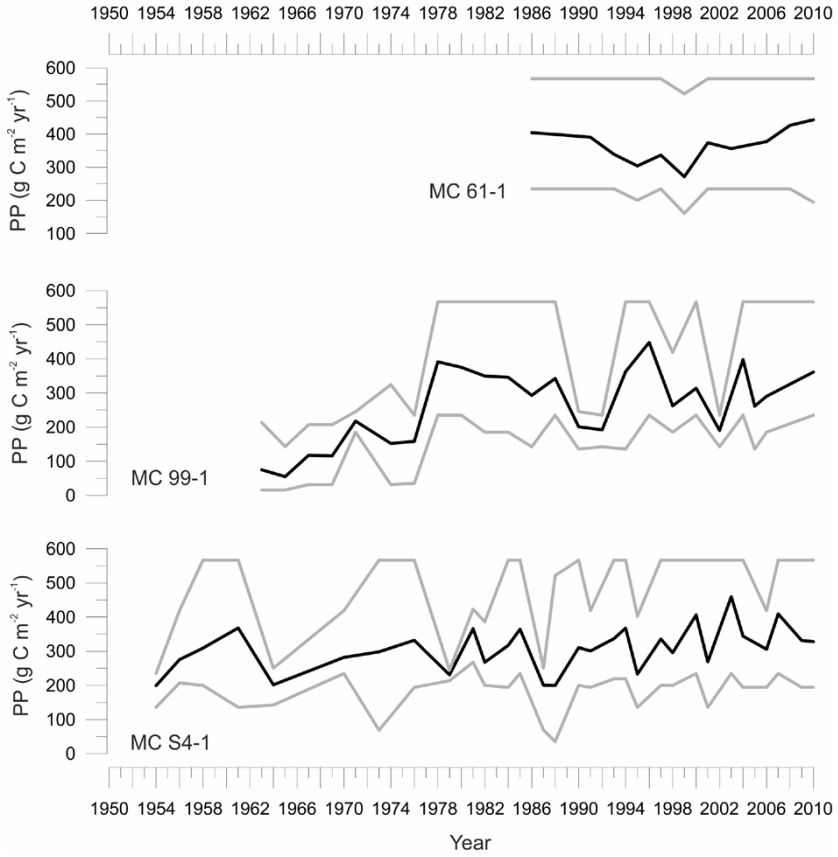

Fig. 10. Reconstructed primary productivity ($g C m^{-2} yr^{-1}$) at every core site; black lines indicate the mean (most probable) values and grey lines the min. and max. values calculated from the set of the 5 selected analogues.

CPD
9, 4553–4598, 2013